Geomechanics and Engineering, Vol. 2, No. 2 (2010) 125-140
DOI: http://dx.doi.org/10.12989/gae.2010.2.2.125

Stability analysis of a rock slope in Himalayas

*Gali Madhavi Latha and Arunakumari Garaga

Department of Civil Engineering, Indian Institute of Science, Bangalore, India

(Received April 15, 2010, Accepted May 20, 2010)

Abstract. Slope stability analysis of the right abutment of a railway bridge proposed at about 350 m above the ground level, crossing a river and connecting two huge hillocks in the Himalayas, India is presented in this paper. The site is located in a highly active seismic zone. The rock slopes are intensely jointed and the joint spacing and orientation are varying at different locations. Static slope stability of the rock slope is studied using equivalent continuum approach through the most commonly used commercial numerical tools like FLAC and SLOPE/W of GEOSTUDIO. The factor of safety for the slope under static conditions was 1.88 and it was reduced by 46% with the application of earthquake loads in pseudo-static analysis. The results obtained from the slope stability analyses confirmed the global stability of the slope. However, it is very likely that there could be possibility of wedge failures at some of the pier locations. This paper also presents the results from kinematics of right abutment slope for the wedge failure analysis based on stereographic projections. Based on the kinematics, it is recommended to flatten the slope from 50^o to 43^o to avoid wedge failures at all pier locations.

Keywords: jointed rock mass; static slope stability; pseudo-static analysis; kinematic analysis and wedge failure.

1. Introduction

Stability analysis of rock slopes becomes essential for the safe design of excavated slopes like open pit mines, road cuts, railway bridges and also to check the equilibrium conditions of a natural slope. Though the knowledge regarding stability analyses and monitoring the slope movement and also the stabilization techniques improved substantially in recent years, rock slope instabilities still extract a heavy social, economic and environmental toll in mountainous regions. This is mainly due to the complexity of the processes driving slope failure and our inadequate knowledge of the underlying mechanisms. Ever increasingly, experts are called upon to analyse and predict the stability of a given slope, assessing its risk, potential mode of failure and possible preventive or remedial measures. Hence the stability assessment of rock slopes considering the influence of all the discontinuities (joints, faults, folds, bedding planes etc.) is a challenging task for engineers.

Though the strength of the rock plays an important role in the slope stability, geological structure of the rock often govern the stability of slopes in jointed rock masses. Geological characteristics of rock mass include location and number of joint sets, joint spacing, joint orientations, joint material and seepage pressure. A rock slope can fail due to one or the combination of these following four

*Corresponding author, Associate Professor, E-mail: madhavi@civil.iisc.ernet.in

mechanisms; circular sliding, plane sliding, wedge sliding and toppling. Circular failure occurs in rock mass which can be justified as homogeneous medium. When the instability is dictated by the presence of pre-existing discontinuities, the failure will be in the form of plane sliding, wedge sliding or toppling, Hoek and Bray (2004). In continuum analysis using graphical or computer methods, the planar failure can be identified. Wedge failure can be identified through stereographic projections of joint planes. To assess the stability of a rock slope, all these possible failure modes need to be checked carefully.

There are several tools available at present to carry out slope stability analyses of jointed rocks and these are well documented by several researchers. Limit equilibrium method used in conjunction with numerical modelling still remains the most commonly adopted method in rock slope engineering, even though most failures involve complex internal deformation and fracturing which bears little resemblance to the rigid block assumptions required by most limit equilibrium back-analyses. Some of the numerical techniques proposed by the earlier researchers include: the shear strength reduction technique developed by Matsui and San (1992), Universal Discrete Element Code (UDEC) developed by Cundall and Strack (1979), Pseudo-static analysis of slope stability proposed by Mononobe and Matsuo (1929) and Okabe (1926). Ling and Cheng (1997) proposed a pseudo-static procedure that determines the seismic factor of safety of a rock mass which slides along a joint plane or along the line of intersection of the joint planes, as a result of earthquake excitation or blasting. These numerical techniques were used by several earlier researchers for various rock engineering applications. Sjoberg (1999) performed numerical analyses of jointed rock masses using UDEC and finite difference program Fast Lagrangian Analysis of Continua (FLAC). Bhasin and Kaynia (2004) performed static and dynamic rock slope stability analyses for a 700-m high rock slope in western Norway using numerical discontinuum modelling technique. Choi and Chung (2004) analysed the stability of jointed rock slopes using Barton-Bandis constitutive model in Discrete Element Code. Chuhan *et al.* (1997) used Distinct Element Method for the dynamic analysis of high rock slopes and block structures.

Kinematic analysis is generally used to evaluate the possibility of blocks or masses of rock moving along geologic structures and sliding out of the face of a slope. The first step in the kinematic analysis is the accurate identification of the features of discontinuities. This is normally done by aerial photographs, surface mapping and examination of borehole cores. Once the discontinuities are mapped, kinematic analysis is usually carried out using graphical stereographic projection approach explained by Goodman (2000) and Philips (1971). Application of kinematic analysis for rock slope stability assessment is also documented well in literature. Some of the applications include Goodman (1995), Leung and Kheok (1987), Yoon *et al.* (2002), Haswanto and Abd-Ghani (2008).

2. Description of the rock slope

A railway line is being laid in the state of Jammu and Kashmir, India and this line is crossing the river Chenab at a height of about 359 m. A bridge is being constructed with a total of 18 piers at this place connecting two big hillocks. Among these piers, 4 piers (P10-P40) are resting on the left abutment and the other 14 piers (P50-P180) are resting on the right abutment. Slope stability analysis of the right abutment is taken up in the present study. The section of the bridge and abutments along with the foundations that could affect the stability of the slope are shown in Fig. 1.

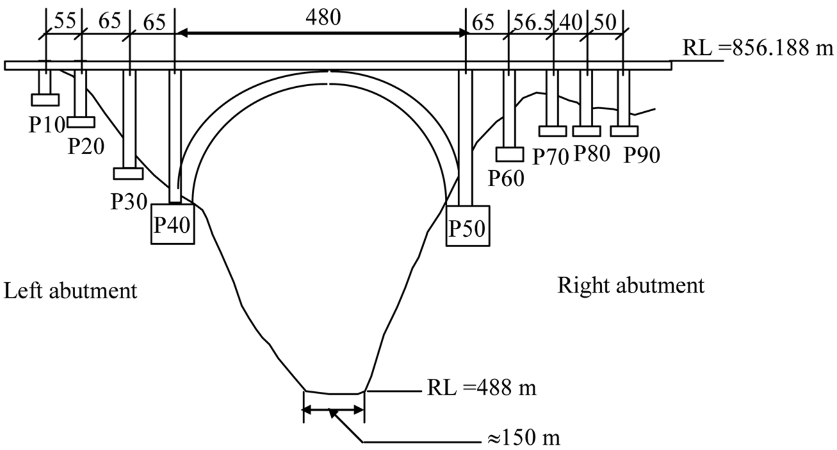

Fig. 1 Section of the gorge with pier foundations along the slope

Fig. 2 Photograph showing the proposed bridge site

Fig. 2 shows the photograph taken at the site of proposed bridge.

The rocks present at the bridge site are heavily jointed. The subsurface at the extent of the bridge site considered for slope stability analysis essentially consists of Dolomitic limestone with different degrees of weathering and fracturing. The main discontinuities at the site are one sub-horizontal foliation joint dipping at about 20~30 degrees in north-east (NE) direction and two sub-vertical joints. The summary of structural features present in the area is given in Table 1. Properties of intact rocks obtained through laboratory testing of cores collected from boreholes at the site are given in Table 2. The original slope has to be cut and benches need to be provided to facilitate the

Table 1 Summary of the structural features at the site

Feature	Strike	Dip	Dip direction
Railway line alignment	N 120° - N 300°	–	–
Foliation joint	N 140° - N 320°	27°	N 50°
Sub-vertical joint -1	N 150° - N 330°	65°	N 240°
Sub-vertical joint -2	N 75° - N 255°	80°	N 165°

Table 2 Properties of intact rock at the site

Property	Value
Density (kg/m^3)	2762
Young's modulus (GPa)	65
Poisson's ratio	0.15
UCS (Mpa)	115
'c' (Mpa) for intact rock	44.44
'ϕ' degrees	35
Hoek and Brown parameters 'm' and 's'	23.52, 1.0

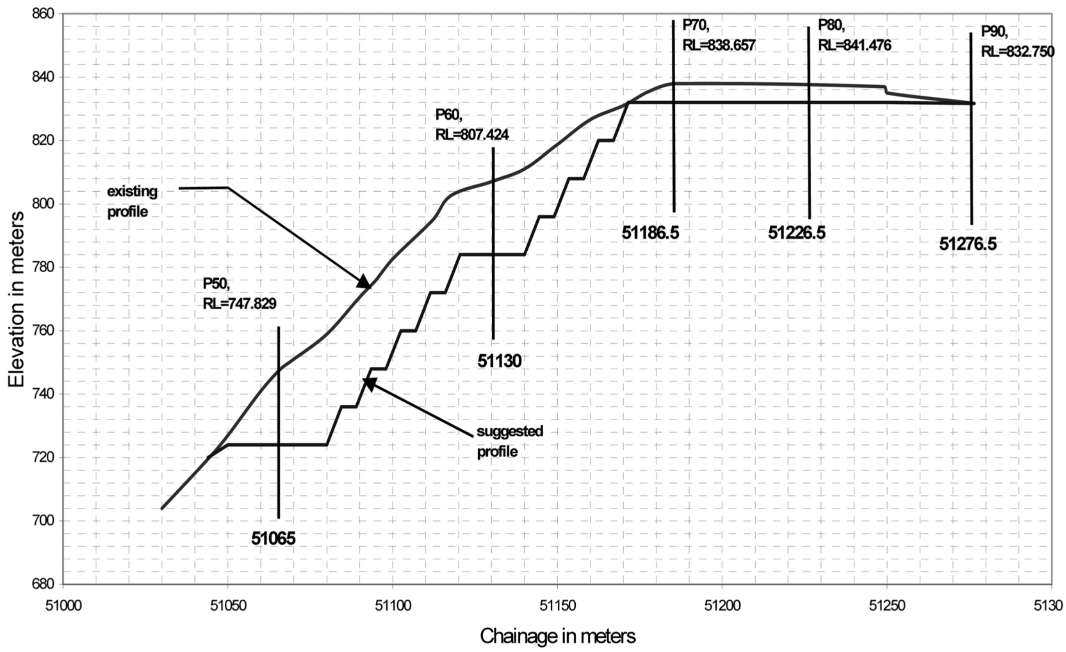

Fig. 3 Profile selected for the stability analysis

construction of foundations along the slope. The outline of benching profile selected for the right abutment is shown in Fig. 3.

Table 3 Rock mass properties used in the stability calculations

Property	Value
Density (kg/m^3)	2762
Young's modulus (GPa)	4.34
Poisson's Ratio	0.15
Hoek and Brown Parameter '*m*'	0.59
Hoek and Brown Parameter '*s*'	0.00127
Cohesion '*c*' (kPa)	1785
Friction angle 'φ' (degrees)	23

3. Static and pseudo-static slope stability analysis of the slope

3.1 Static slope stability analysis by FLAC

The slope is simulated using FLAC (Fast Lagrangian Analysis of Continua) version 5.0 developed by Itasca consulting group (1995). FLAC is a widely used commercial, explicit finite difference code for applications in soils and rocks. It is impossible to incorporate and model all the discontinuities in large slope in a numerical model as the joints are spaced very close (joint spacing varying between 5 mm to 10 mm). Hence the slope is represented by an equivalent continuum in which the effect of discontinuities has been considered by reducing the properties and strength of intact rock to those of the rock mass. The slope is analysed for plane-strain condition in small-strain mode. A relatively finer discretization of 100×80 grid size is chosen for modelling the slope. At the base of the model boundary, both horizontal (x) and vertical (y) displacements are arrested by fixing the nodes. Along left and right of the boundary horizontal displacements are arrested. Initial stresses of magnitude $\sigma_{xx} = \sigma_{yy} = \sigma_{zz} = 8$ MPa are applied to all the zones. Stability analysis is carried out using Hoek-Brown failure criterion in FLAC. FLAC calculates the factor of safety automatically using the shear strength reduction technique through bracketing (Matsui and San 1992). In this technique, the values of shear strength parameters 'c' and 'ϕ' are updated in every trial until the difference between lower and upper brackets is minimal according to the following equations.

$$c_{trial} = \frac{1}{F_{trial}} \times c \tag{1}$$

$$\phi_{trial} = \tan^{-1}\left[\frac{1}{F_{trial}} \tan\phi\right] \tag{2}$$

The value of 'F_{trial}' at which slope will have instability *i.e.* failure is calculated by *FLAC* using the bracketing technique. Initially upper and lower brackets are established. The initial lower bracket is any 'F_{trial}' for which a simulation converges. The initial upper bracket is any 'F_{trial}' for which the simulation does not converge. Next, a point midway between the upper and lower brackets is tested. If the simulation converges, lower bracket is replaced by this new value. If the simulation does not converge, the upper bracket is replaced. The process is repeated until the difference between the upper and lower brackets is less than a specific tolerance.

The analysis is carried out with and without pier loads. Properties of the rock mass used in the

Table 4 Details of the footing pressures

Property	P50	P60	P70	P80	P90
Chainage (km)	51.065	51.13	51.1865	51.2265	51.2765
Original ground level (m)	747.829	807.421	838.657	841.476	832.750
Ground level after benching (m)	724	784	832	832	832
Depth of foundation (m)	3	3	3	3	7
Foundation size (m × m)	28 × 36	11 × 9.5	11 × 6.5	11 × 6.5	11 × 6.5
Footing Pressure (kPa)	374.86	588.00	409.00	415.00	317.00

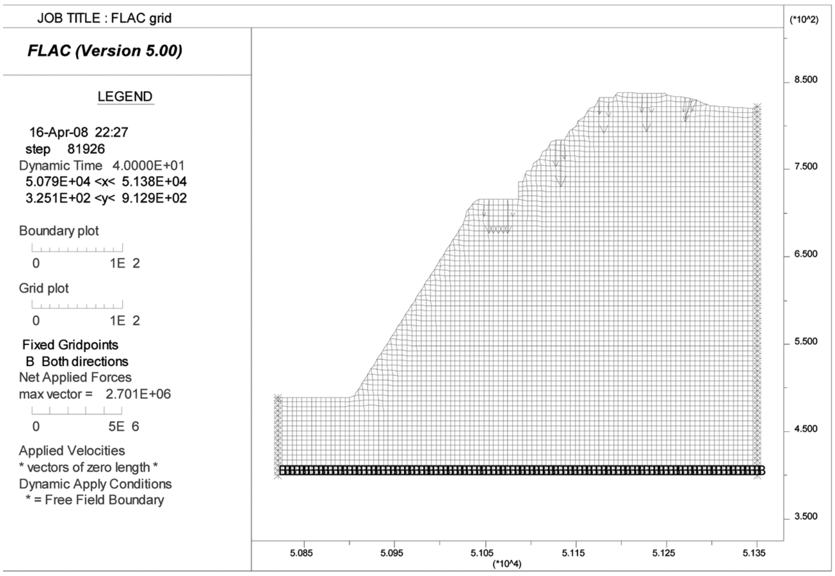

Fig. 4 FLAC grid used for the stability calculations

stability calculations are shown in Table 3. These are the average values obtained by laboratory tests on jointed rock mass collected at different pier locations. Table 4 presents the values of pier loads applied on the slope at respective pier locations. Fig. 4 shows the finite difference grid generated in FLAC for using in the stability calculations. The results obtained from the stability analysis on the cut profile are shown in Fig. 5 in the form of FOS (Factor of Safety) plot. The value of FOS obtained from the static analysis is 1.88 which means that the slope is globally stable. Fig. 6 shows the plastic zone for the cut profile with pier loads. It is clear from Fig. 6 that tension is occurring at the crest indicating yielding. Stability analysis was also carried out on cut profile without pier loads and it was noticed that the value of factor of safety is not altered greatly with the pier loads, showing that the effect of pier loads is insignificant on the overall stability of the slope. The reason for this is that the magnitude of the pier loads is very less when compared to the overall weight of the slope.

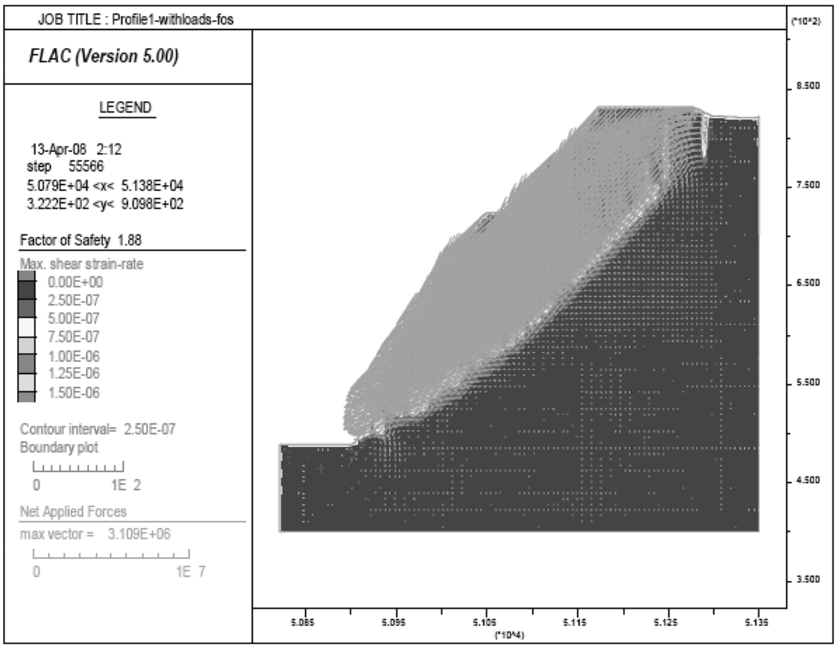

Fig. 5 Factor of safety plot for the static stability of rock slope

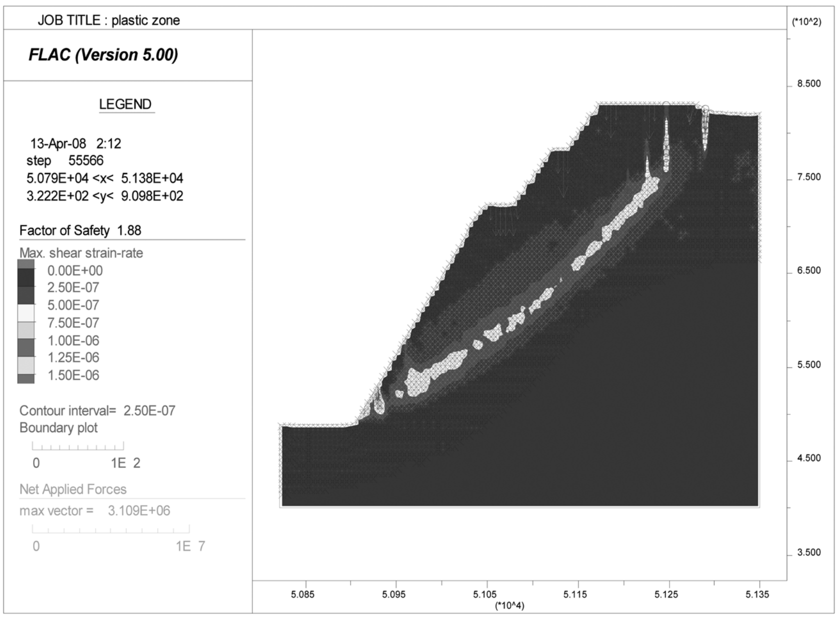

Fig. 6 Plastic zone for cut profile with pier loads (k_H=0.31 g, k_v=0.2 g)

3.2 Static slope stability analysis by SLOPE/W of GEOSTUDIO

The same slope is modelled in SLOPE/W of GEOSTUDIO. SLOPE/W is a popular software for

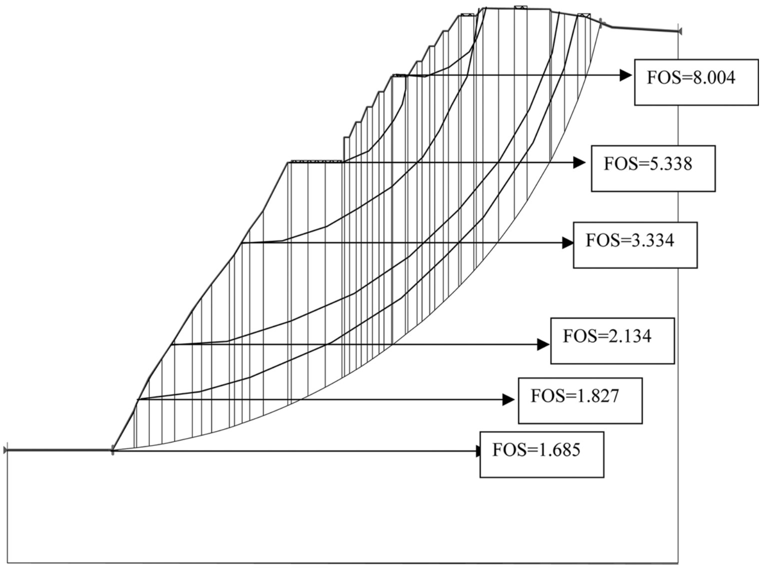

Fig. 7 Trial failure surfaces and corresponding factors of safety

computing the factor of safety of earth and rock slopes. Using limit equilibrium approach, SLOPE/W can model heterogeneous soil types, complex stratigraphic and slip surface geometry, and variable pore-water pressure conditions using a large selection of soil models. Stresses computed by a finite element stress analysis may be used in addition to the limit equilibrium computations for the most complete slope stability analysis available. With this comprehensive range of features, SLOPE/W can be used to analyze almost any slope stability problems in geotechnical, civil, and mining engineering projects. For the right abutment slope, SLOPE/W analyses have been carried out using ordinary method of slices to obtain minimum factors of safety for the critical slip surfaces based on iterative techniques. The FOS values computed from SLOPE/W are used to cross check the values of factors of safety obtained from FLAC.

3.3 Check for local stability of slope at pier locations

In order to check the stability against local failures, various slip surfaces were considered for the slope passing through various pier locations and the minimum factors of safety for these slip surfaces are obtained using SLOPE/W with ordinary method of slices. Fig. 7 shows these slip surfaces and corresponding factors of safety obtained from the limit equilibrium analysis. As anticipated, it is observed that as the size of the slip surface is reduced, the factor of safety is increased and the minimum factor of safety was obtained for the slip surface passing through the toe.

3.4 Pseudo-static slope stability analyses

Slope failure and landslides are mainly caused due to the earthquake induced ground shaking and associated inertial forces. Earthquakes with even a very small magnitude may trigger failure in slopes which are perfectly stable otherwise. As the slope under consideration is situated in seismic zone *V* of India, where severe earthquakes are expected, it is mandatory to assess the stability of the

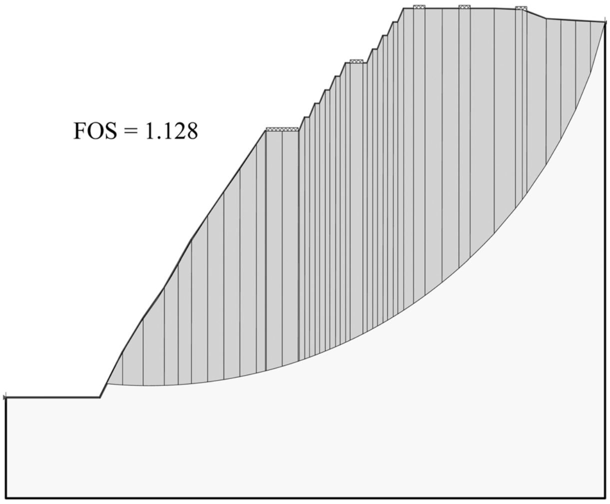

Fig. 8 Factor of safety plot for the slope with pier loads and seismic loads obtained from SLOPE/W (k_H and k_V are applied)

slope under seismic conditions. The seismic slope stability is estimated using pseudo-static approach (Mononobe and Matsuo 1929, Okabe 1926).

Pseudo-static analysis involves simulating the ground motion as constant static horizontal force acting in a direction out of the face. The analysis represents the effects of earthquake shaking by pseudo-static accelerations that produce inertial forces, 'F_H' and 'F_V' which act through the centroid of the failure mass. The magnitude of the pseudo-static force is the product of seismic coefficient 'k_H' and the weight of the sliding block 'W'. The value of 'k_H' may be taken as equal to the design *PGA* (Peak Ground Acceleration) which is expressed as a fraction of the gravity acceleration. The horizontal pseudo-static force decreases the factor of safety by reducing the resisting force (for $\phi > 0$) and increases the driving force. The vertical pseudo-static force typically has less influence on the factor of safety since it reduces (or increases, depending upon the direction) both the driving force and the resisting force, as a result the effect of vertical accelerations are usually neglected in pseudo-static analyses. However the effect of vertical acceleration is also considered in the present study. The horizontal pseudo-static forces are assumed to act in directions that produce positive driving moments. Results of the pseudo-static analysis critically depend upon the horizontal seismic coefficient (k_H). Therefore selection of appropriate pseudo-static coefficient is very important. Usually this value is selected based on the Most Credible Earthquake (MCE) for the specific seismic zone in which the slope is situated. In the present study, the horizontal seismic coefficient 'k_H' is selected as 0.31 g based on the previous earthquake history of the region and MCE scenario. The value of the vertical seismic coefficient 'k_V' is taken as 2/3rd of 'k_H' as per the Indian Standard Code IS 1893 (2002). The analysis is carried out for two different cases *i.e.* considering the horizontal seismic force component (k_H) alone in the first case and by applying both vertical and horizontal components (k_H and k_V) in the second case. Pseudo-static analysis of the slope is carried out using both SLOPE/W and FLAC.

The result obtained from SLOPE/W is shown in Fig. 8 along with the FOS value. Figure shows the FOS value considering both horizontal as well as vertical components of earthquake. The value of FOS obtained is 1.128. Similarly the results obtained from pseudo-static analysis of the slope in

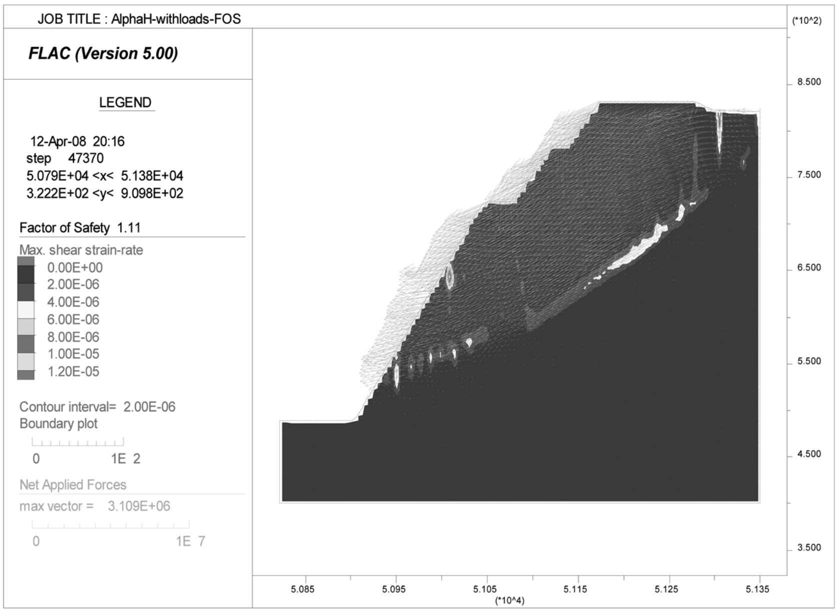

Fig. 9 FOS plot for the slope using pseudo-static approach obtained using FLAC (k_H alone is applied)

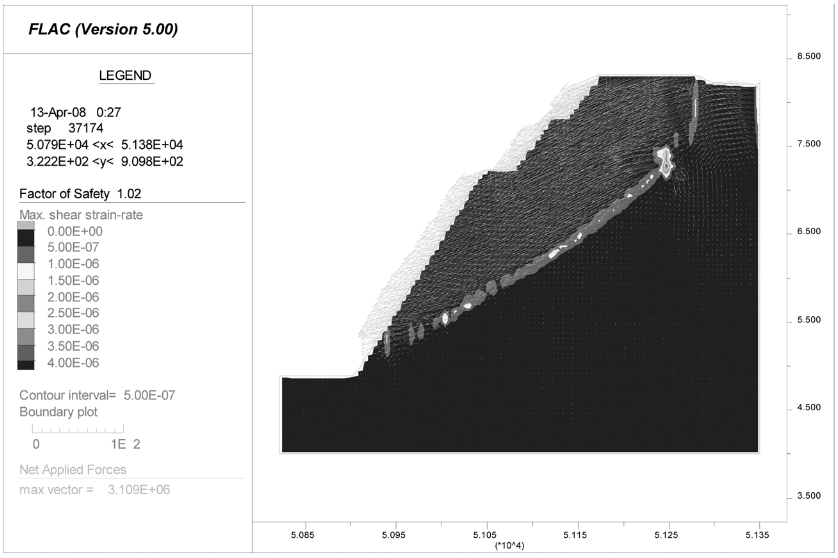

Fig. 10 FOS plot for the cut profile using pseudo-static approach ('k_H' and 'k_V' are applied)

FLAC are shown in Figs. 9 and 10. Fig. 9 gives the *FOS* plot for the slope considering only horizontal seismic force component. The factor of safety obtained for this case was 1.11. Fig. 10 gives the *FOS* plot for the slope with both horizontal and vertical seismic force components. The value of *FOS* for this case was reduced to 1.02.

Factor of safety for the slope without considering earthquake loads was 1.89. By applying the horizontal earthquake force alone, the FOS is reduced to 1.11 and with the application of vertical

Table 5 Factors of safety values obtained from slope stability analysis

Profile	Without earthquake loading		With earthquake loading ($k_h = 0.31$ g)		With earthquake. loading ($k_h = 0.31$ g, $k_v = 0.2$ g)	
	SLOPE/W	FLAC	SLOPE/W	FLAC	SLOPE/W	FLAC
Original Slope	1.920	1.880	–	–	–	–
Benched profile	1.829	1.900	1.128	1.110	1.128	1.023

Table 6 Details of joints at different locations along the slope

Location	Joint set J_1		Joint set J_2		Joint set J_3		Joint set J_4	
	Dip	Dip Direction	Dip	Dip Direction	Dip	Dip Direction	Dip	Dip Direction
Valley	42°	049°	52°	238°	72°	151°	15°	336°
P70	67°	047°	47°	244°	70°	131°	51°	263°
P60	40°	049°	56°	240°	69°	153°	39°	308°
P50	40°	054°	48°	234°	71°	153°	08°	032°

earthquake force it is further reduced to 1.02. Earthquake loads reduced the FOS by 46%. The minimum FOS required for rock slopes considering the earthquake loads is 1.2. But the factor of safety obtained from pseudo-static analysis considering both horizontal and vertical loads is falling below the required *FOS* value. However it is noteworthy to mention that the pseudo-static analysis is a highly conservative method because it is performed with continually applied seismic forces in horizontal and vertical directions, which is not realistic. For this analysis, as FOS value of 1.0 is acceptable as per NEHRP guidelines for land sliding hazards. Hence the slope can be considered as globally stable under seismic loading conditions as well.

The factors of safety obtained from static and pseudo-static slope stability analyses using both FLAC and SLOPE/W are summarised in Table 5.

4. Kinematics of slope stability for wedge failure analysis

In the previous section of this paper, global stability of the slope is examined through static and pseudo-static slope stability analysis and it was found that the slope is stable in both static and probable seismic conditions. However, the global failure is a rare possibility for this slope under consideration. Though the overall stability is understood, it is very much essential to investigate the possibility of local wedge failures which might occur due to the intersection of joint sets daylighting on to the slope. The possibility of wedge failure at different pier locations is examined in this section by plotting stereographic projections for the prevailing joint sets in the bridge site. The geological data of joint sets for the stereographic projections is obtained from the joint mapping done by the geologists from the exposed slope surface at different pier locations.

4.1 Stereographic projection of joints for the right abutment

The geological data regarding the dip and dip direction of various joint sets at different pier

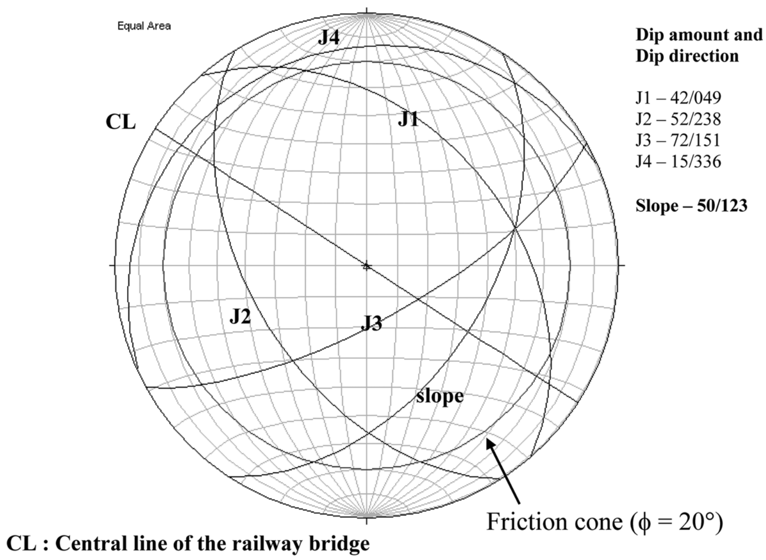

Fig. 11 Stereographic projections of joints at valley portion

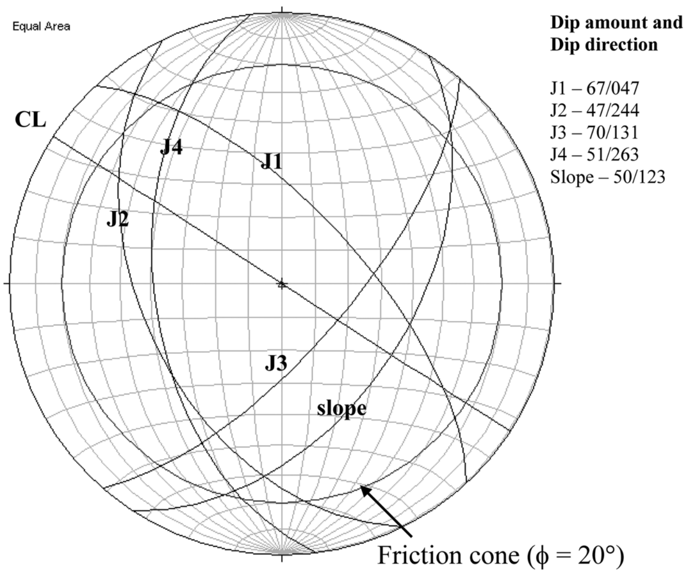

Fig. 12 Stereographic projections of joints at S70

locations obtained form the geological mapping at the slope site is presented in Table 6. Using the data in Table 6, stereographic projections of joint sets are plotted for various locations. The average angle of slope for the right abutment of the bridge is 50^{o} and the corresponding dip direction is 123^{o}. Stereographic projections of joint sets at valley portion, P70, P60 and P50 are shown in Figs. 11, 12, 13 and 14 respectively.

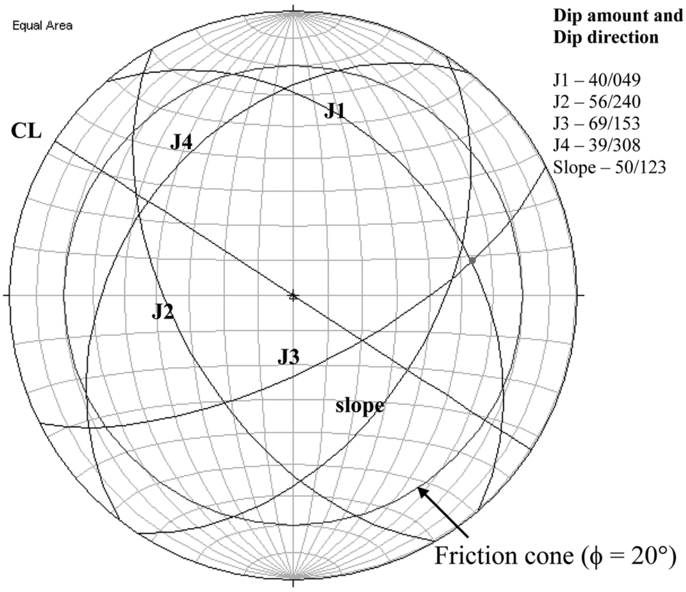

Fig. 13 Stereographic projections joints at S60

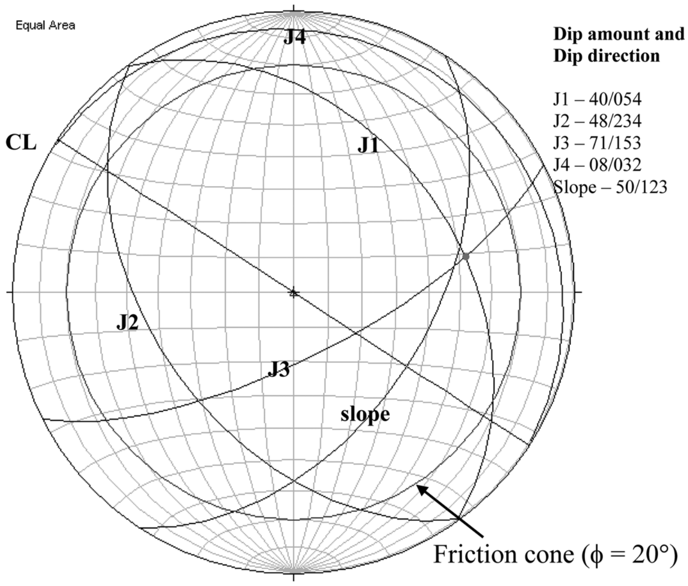

Fig. 14 Stereographic projections of joints at S50

4.2 Analysis for wedge failure

Wedge failure occurs due to sliding along a combination of discontinuities. The conditions for sliding require that the friction angle of the rock mass 'ϕ' is overcome, and that the intersection of the discontinuities "daylight" on the slope surface. On the stereonet plot, these conditions are

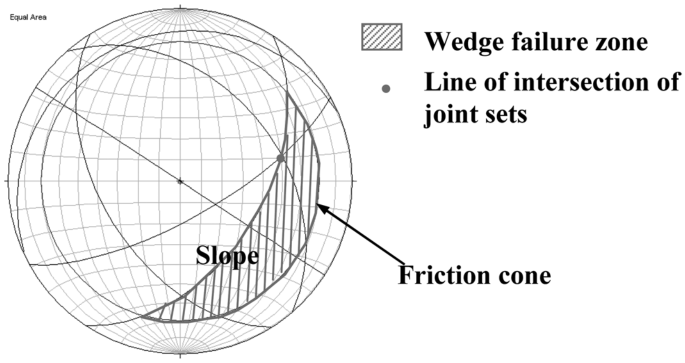

Fig. 15 Condition for wedge failure

Fig. 16 Wedge failure observed in exploratory drift at P50

indicated by the intersection of two discontinuity great circles within the shaded crescent formed by the friction angle and the slope's great circle as shown in Fig. 15.

Based on the stereographic projections with slope angle of 50^o, it is seen that wedge failure is possible at valley, P60 and P50 locations as the line of intersection of joint sets 'J_1' and 'J_3' is falling in the crescent formed by the slope angle and friction angle. Wedge failure is in fact occurred during excavation of exploratory drift at P50 as shown in Fig. 16, supporting the stereographic interpretations that the wedge failures are possible in this zone.

It is observed that the friction angle reported from the laboratory tests is very low (about 20^o). However, increase in the value of friction angle will not arrest the wedge failures as it could be seen from the stereographic plots that the line of intersection of joints in the crescent is close to the slope rather than the friction cone. Hence to avoid the wedge failures at the above mentioned locations (Valley, P50 and P60), the slope needs to be flattened. By plotting the stereographs for slope angle of 45^o, it was observed that the wedge failure is still possible at P60. By trial, it was observed that the maximum permissible value for slope is 43^o to avoid wedge failures at all the locations and the results are presented comprehensively in Fig. 17.

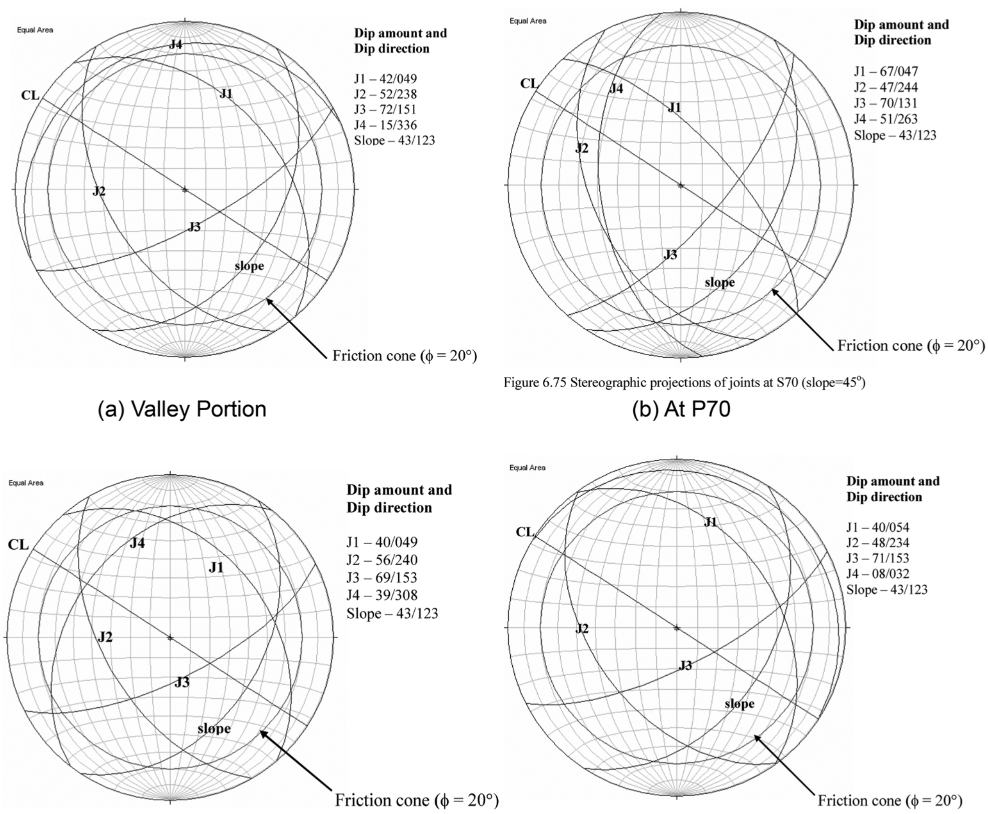

(a) Valley Portion (b) At P70

(c) At P60 (d) At P50

Fig. 17 Stereographic projections of joints at different locations for flattened slope of 43°

5. Conclusions

A case study of large slope in Himalayan region of India is taken up in this paper and numerical analysis of the slope is carried out using the equivalent continuum approach. The slope is analyzed for stability under static and seismic loading conditions. Calculation of Factor of safety for the slope in static and pseudo-static conditions confirmed the global stability of the slope in static and pseudo-static conditions. The factor of safety for the slope under static conditions was 1.88 and by applying the horizontal earthquake force alone, the FOS is reduced by 40%. With the application of vertical earthquake force it is further reduced by another 6%. Probability of wedge failure is assessed through kinematic analysis of the slope by drawing stereographic projections of joint planes prevailing in the bridge site and the slope. Based on the kinematics, it is recommended to flatten the slope from 50° to 43° to avoid wedge failures at all pier locations.

References

Bhasin, R. and Kaynia, A.M. (2004), "Static and dynamic simulation of a 700 m high rock slope in western

norway", *Eng. Geol.*, **71**, 213-226.
Choi, S.O. and Chung, S. (2004), "Stability analysis of jointed rock slopes using the Barton-Bandis constitutive model in UDEC", *Int. J. Rock Mech. Min. Sci.*, **41**(1), 581-586.
Cundall, P.A. and Strack, O. D. (1979), "A discrete numerical model for granular assemblies", *Geotechnique*, **21**, 47-65.
Goodman, R.E. (1995), "Block Theory and its application", *Geotechnique*, **45**(3), 383-423.
Goodman, R.E. (2000), *Introduction to Rock Mechanics*, John Wiley & Sons, New Jersey, USA
Haswanto, W.A. and Abd-Ghani, R. (2008), "Kinematic and block theory applications to rock slope stability analysis at Fraser's hill Pahang Malaysia", *Electron. J. Geotech. Eng.*, **13**(D).
Hoek, E. and Bray, J. (2004), *Rock Slope Engineering*, Ed. D.C. Wyllie and C.W. Mah, Taylor and Francis, London, UK.
IS 1893 (2002), *Criteria for earthquake resistant design of structures*, Bureau of Indian Standards, New Delhi, India.
Itasca (1995), *FLAC Version 5. User's Manuals*, Itasca Consulting Group, Minnesota, USA.
Leung, C.F. and Kheok, S.C. (1987), "Computer aided analysis of rock slope stability", *Rock Mech. Rock Eng.*, **20**, 111-122.
Ling, H.I., Alexander, H. and Cheng, D. (1997), "Rock sliding induced by seismic force", *Int. J. Rock Mech. Min.*, **34**(6), 1021-1029.
Matsui, T. and San, K.C. (1992), "Finite element slope stability analysis by shear strength reduction technique", *J. Soils Found.*, **32**(1), 59-70.
Mononobe, N. and Matsuo, H. (1929), "On the determination of earth pressures during earthquakes", *Proceedings of World Engineering Conference*, Tokyo, Japan, Vol. IX, Paper No. **388**, 177-185.
Okabe, S. (1926), "General theory of earth pressure", *J. JPN Soc. Civil Eng.*, **12**(1), 311.
Phillips, F.C. (1971), *The use of Stereographic Projections in Structural Geology*, Edward Arnold, London, UK.
Sjoberg, S. (1999), *Analysis of large scale rock slopes*, Doctoral Thesis, Department of Civil and Mining Engineering, Lulea University of Technology, Sweden.
Yoon, W.S., Jeong, U.J. and Kim, J.H. (2002), "Kinematic analysis for sliding failure of multi-faced rock slopes", *Eng. Geol.*, **67**, 51-61.
Zhang, C. Pekau, O., Jin, F. and Wang, G. (1997), "Application of distinct element method in dynamic analysis of high rock slopes and blocky structures", *Soil Dyn. Earthq. Eng.*, **16**, 385-394.

CC